VOL.3 NO.2September 2014 - ISSN 2233 – 1859

Operations Research Society in Bosnia and Herzegovina

Southeast Europe Journal of Soft Computing

Available online: www.scjournal.com.ba

IUS Soft Computing Research Group

New Pose Estimation Methodology for Target Tracking and Identification

Part I. Target Signatures and Hypothesis Testing

Migdat I. Hodzic, Tarik Namas
International University of Sarajevo, FENS, Sarajevo, Bosnia and Herzegovina
mhodzic@ius.edu.ba, tnamas@ius.edu.ba

Article Info

Article history:
Received Sep 2014
Received in revised form Nov 2014

Keywords:
Target Tracking and Identification, Pose Estimation, Automatic Target Recognition, Statistical Hypothesis Testing

Abstract

Ground Moving Target Indicator (GMTI) and High Resolution Radar (HRR) can track position and velocity of ground moving target. Pose, angle between position and velocity, can be derived from kinematics estimates of position and velocity and it is often used to reduce the search space of a target identification (ID) and Automatic Target Recognition (ATR) algorithms. Due to low resolution in some radar systems, the GMTI estimated pose may exhibit large errors contributing to a faulty identification of potential targets. Our goal is to define new methodology to improve pose estimate. Besides applications in target tracking, there are numerous commercial applications in machine learning, augmented reality and body tracking.

1. INTRODUCTION

With high-resolution radar sensors such as HRR and SAR (Synthetic Aperture Radar), ground targets become visible more as a rich set of radar signatures corresponding to the target geometrical details than as a single reflector with an equivalent RCS (Radar Cross Section). Feature and signature aided tracking and ATR applications benefit from HRR radar processing. Successful simultaneous tracking and identification applications exploit feature information to determine the target type and dynamics. This has enabled target classification and identification (ID), as well as ATR. As a "by-product" of the target ID/ATR process, the pose angle estimates are available. Pose information consists of a depression angle and an aspect angle (Fig. 1). The depression angle is related to the sensor position and aspect angle can be determined from the HRR profile. For ground targets, which are constrained to move on the earth surface, their velocity vector direction is aligned most of time along the body's longitudinal axis. As a result, the pose angles carry kinematic information that can be used to aid target tracking particularly during the maneuvering periods. See more in [1],[2],[4],[5] and [6]. In this paper we present a methodology for a better pose estimate algorithms, which can in turn accomplish improved target tracking and identification, as well as reduce target miss-association probability (MAP). To maximize a search area, airborne systems operate at standoff ranges to detect targets and initiate tracks. Tracking systems then transition into a track maintenance mode after target acquisition; however, closely spaced targets such as at road intersections require feature analysis to identify the targets. HRR radar affords dynamic processing analysis for vehicle tracking and signal features (range, angle, aspect, and peak amplitudes) for target detection and identification. Pattern recognition algorithms applied to ATR problems are typically trained on a group of desired objects in a library to gain a statistical representation of each objects' features. In this paper we propose to use new statistical comparison approach based on novel idea of combining several statistical methods which uses off line generated template against real HRR target signature data. We exploit time, frequency and correlation features of the HRR signatures. The algorithm then aligns real time signatures to the library templates of targets and determines the best correlation value for the aligned features. In doing so we propose classic methods

of Pearson and Spearman coefficients as well as chi square testing. Also, a new methodology via Haar Transform [24] and recently introduced statistical method of Brownian Distance Correlation [27] are considered as well. Based on these methods, various statistics of the outputs are compared and cross-correlation among two sets of data (stored and real) is calculated. In order to match and choose target pose angle, we will employ statistical hypothesis testing which will result in improved pose estimate. In Part II of this paper, we determine and predict performance of coupled target tracker and identifier as a function of pose estimate. Target tracking will be implemented using multiple Extended Kalman Filters (M-EKF) or Unscented Kalman Filters (M-UKF) in Cartesian coordinates with nonlinear (polar) measurements including pose (or just aspect) angle. Each filter handles one target type, produces estimates in continuous space kinematics, and is associated a probability of being used, which determines target probability as well. Pose sensitivity to parameter changes will be analyzed also.

Besides defense applications, results in this paper can be used in Intelligent Vehicle Highways, Intersection Traffic Control, Benefits are (i) improved traffic flow, (ii) increased safety and (iii) improved gas mileage. Additional applications are in the area of Augmented Reality, Facial Features estimation.. and Machine Learning algorithms development.

2. TECHNICAL OBJECTIVES SUMMARY

The overall objective of this paper is to introduce a methodology to develop better pose estimation technique, improve coupled tracking-identification process, and reduce target miss-association. We will use a case - study of well known USA Air Force airborne platform of JSTAR [4], [5]. The platform is based on old Boeing 707 aircraft that has been fitted with many sophisticated target identification and tracking equipment. JSTAR has seen deployments in Bosnia to enforce Dayton Peace Agreement, and Kosovo, among other places, in mid and late 1990s. There is a current JSTAR modernization effort under way.

The objectives of this paper are listed below. In Part I of this paper, we cover first three objectives, while remaining three will be covered in Part II.

1. Target Signature Profiles. Present new approach for generating spatial and frequency target data templates obtained from raw and digitized HRR (SAR) data. The data can be derived from public Moving and Stationary Target Acquisition and Recognition (MSTAR) program database. The MSTAR data consists of SAR data (X-band l x 1 foot resolution). Once real time target raw signature is obtained, it will be discredited and stored in a form as any of the template entries, Table 1.

2. **Target Signature Statistics**. Define effective and less computationally intensive ID/ATR search and registration process which uses statistical comparison of off line analyzed HRR template data, step 1 above, and HRR target data obtained in real time. The key requirement here is that the process is fast and computationally simple so it can be done in real time, when many 1000s of templates are scanned and compared. We propose to use new techniques in spatial and frequency domains, as well as some new and classic correlation methods, all aimed at identifying weak or strong target signature correlations.

3. Target Hypothesis Testing. Once various target signature statistics are generated in Objective 2 above, we proceed and perform a variety of hypothesis testing cases, to identify strong and weak correlations between real time signature and template signatures stored ahead of any real time operation. This is very important step and it results in an estimate of the most likely pose angle, based on real time vs. template match. Note that the best match would correspond to a rough pose angle estimate from Table 1, or maybe a narrow range of pose angles. This all leads us to Objective 4 bellow.

4. Pose Angle Estimate. Good pose estimate (depression and aspect angles, φ and ϕ) accomplishes reduction in probability of real time target miss - association, which allows for the capability to discern relevant targets and reject non-plausible targets. Radar tracking assumes that after receiving the energy return from the target, the approximate coarse position of the target results. Since a finite number of range bins are collected, the center bin is assumed to be the position of the target (see Fig. 2 and 3 bellow). Additionally, the radar data has an associated depression and azimuth angle to the target, see Fig. 1 hence further pose estimate fine tuning will be done with the help of the results of Objective 5.

5. Target Tracking. With a rough pose angle estimate we define a bank of parallel target tracking filters, each one for a particular target type. The MTI (SAR) radar combined with a monopoles radar processing provides the measurements of Range (r), Range rate (dr/dt), Azimuth angle (α) and also Elevation angle (ε), from the aircraft to the target (Figure 1). The HRR provides a target range profile from which we can deduce the pose estimate, i.e. depression and aspect angles. Typically this reduces to just aspect angle because the depression angle is kept fixed, as it will be assumed throughout the work here. Hence we will have two rough pose estimates to work with, and to improve on.

6. Sensitivity Analysis. Predict the performance (better or worse) of target identifier and tracker due to pose estimate quality. This step corresponds to calculating sensitivity of identification (or, in turn, target miss-association) and tracking performance with respect to pose estimate. We will calculate the sensitivity of various statistical parameters to probability of miss – association and identify less sensitive and more sensitive parameters from the steps above. This corresponds to breaking down pose sensitivity calculation, into individual calculations of statistical parameters and signature profiles.

3. TARGET SIGNATURE PROFILES

Our methodology consists of six steps (3 in Part I, 3 in Part II), for six technical objectives of Section II. We start with:

STEP 1. Develop target signature profiles

1.1 Obtain row and digitized data for all template targets of interest. We can use public domain MSTAR, or other sources. Table 1 shows N targets and M pose angles. To each entry we add SFs, AFs, and FFs, all ahead of time

1.2 Get row and digitized signature for a real time target.

It is in the same form as any Table 1 entry. We assume this is done in real time on JSTAR or similar platform.

TABLE 1. HRR TEMPLATE PROFILE

Pose Target	Pose 1	Pose 2	..	Pose M	Features / Statistics
Target 1	Template (1,1)	Template (1,2)	..	Template (1,M)	F/S Set 1
Target 2	Template (2,1)	Template (2,2)	..	Template (2,M)	F/S Set 2
.....	.....	.....	..	.....	…..
Target N	Template (N,1)	Template (N,2)	..	Template (N,M)	F/S Set N

The MSTAR data consists of SAR data in X band, l x1 foot resolution. Images are recorded at 15°and 17° depression angles with aspect angle 360°range, at around 1°spacing in azimuth. The methodology used to convert the SAR imagery to HRR is discussed in [15]. While the MSTAR data consists of all aspect data, for each measurement pose estimate, viewing aspect angles considered are -5°<φ< 5°in azimuth and 15°and 17°in depression angle. Each HRR image results in 101 HRR profiles, which represent approximately a 3°variation in azimuth. If we have 50 target types, that is a total of 5,050 signature profiles, plus additional statistical data (last column in Table 1) as described in Section IV.

In Steps 1.1 and 1.2, we form specific Spatial, Amplitude and Frequency Signature Feature vectors.

Spatial Features (SFs) consist of:

- Row HRR data (MSTAR or other source), Fig. 2.
- Vector of K digitized raw data, Fig. 3. Here K = 16 for the purposes in this paper. In real situations, digitization is done by a professional equipment, and the number of points could be 32, 64, 128 or more, case specific. The number of points is $K = 2^m$, m=1,2,3,… .

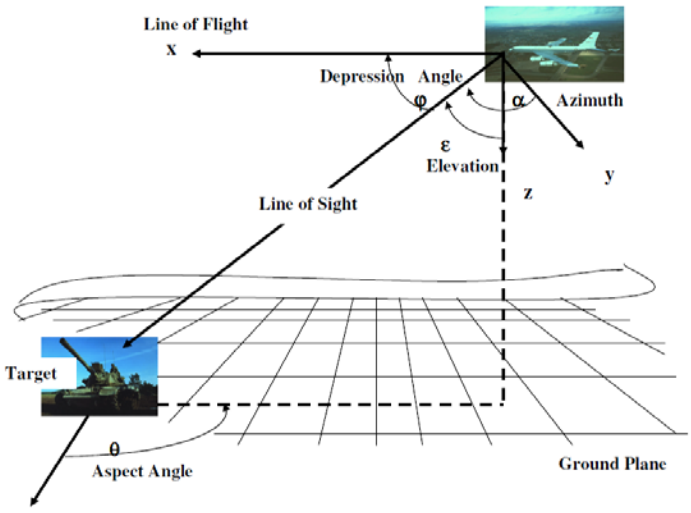

Figure 1. HRR and MTI Radar Geometry

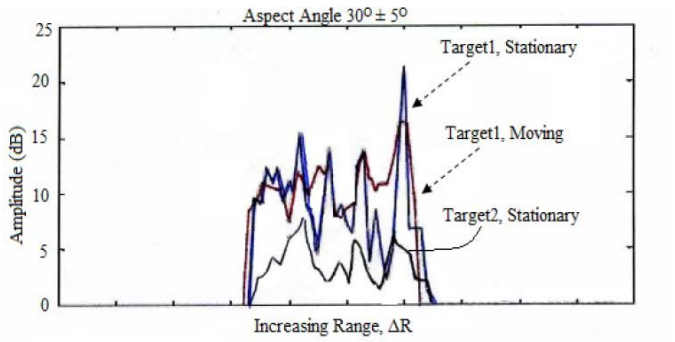

Figure 2. Continuous HRR Range Data Over ΔR Stationary Target 1 and 2, and Moving Target 1 Signatures

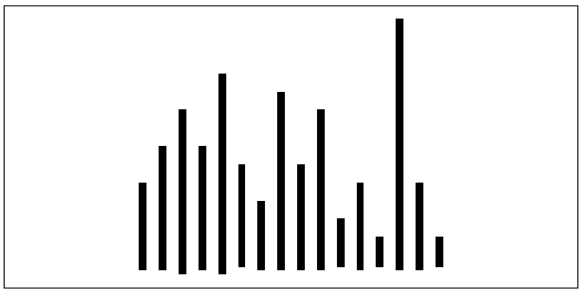

Figure 3. Digitized Data, Stationary Target 1, Fig. 2 Each Vertical Line is one digitized range bin

Besides Spatial Features, we define several derived signal characteristics. These include Amplitude Features (AFs) and Frequency Features (FFs), all localized to the total range span ΔR indicated in Fig. 2.

Amplitude Features (AFs) vector, formed of statistics:

- Highest amplitude (A_{max}) (or two highest ones)
- Lowest amplitude (A_{min}) (or two lowest ones)
- Average signal amplitude (A_{av})
- Median amplitude value (A_{med})
- Standard deviation (A_{sd})

plus such indicators as:

- Ratio (A_{max}/A_{min})
- Total energy (A_e), as the sum of amplitudes squared
- Number of discretized peaks and valleys (A_p), (A_v)

A_p = Number of Low-High-Low cases

A_v = Number of High-Low-High cases = A_p-1

Note that in order to be very precise about the AFs, we would need more than 16 sampling points, hence we need to keep that in mind in our results and discussions here.

Frequency Features (FFs) vector generated by using:

- Haar Transform Matrix operating on SF vector, such as in Equation 5 and Tables 2, 3 and 4 in Section 6.

The Haar transform is very useful in signal processing applications where real-time implementation is essential. The Haar transform is based on Haar functions which are periodic and orthogonal. The Haar functions become increasingly localized as their number increases [24], which provides frequency domain in which signature energy is concentrated in localized regions. This property is very useful in various applications.

The Haar transform matrix is an orthogonal one, hence the inverse Haar transform can be derived from:

$$HH^T = I, \quad H^{-1} = H^T \tag{1}$$

where I is the identity matrix. The 1st order Haar matrix is:

$$H(1) = 1/\sqrt{2^1} \text{ times} \tag{2}$$

1	1
1	-1

The recursive equation for higher order Haar matrices [ ] is:

$$H(k+1) = 1/\sqrt{2^{k+1}} \text{ times} \tag{3}$$

H(k)*[I I]
$2^{k/2}$ I(2^k)*[I –I]

where "*" is Kronecker product [ ], I(2^k) is Identity matrix of order 2^k, such that H(2) is 4x4, H(3) is 8x8, and H(4) is 16x16 matrix, and so on. Take the 8x8 Haar matrix H(3):

$$H(3) = 1/\sqrt{2^3} \text{ times} \tag{4}$$

1	1	1	1	1	1	1	1
1	1	1	1	-1	-1	-1	-1
√2	√2	-√2	-√2	0	0	0	0
0	0	0	0	√2	√2	-√2	-√2
2	-2	0	0	0	0	0	0
0	0	2	-2	0	0	0	0
0	0	0	0	2	-2	0	0
0	0	0	0	0	0	2	-2

Unlike Fourier transform, Haar transformation invilves only real numbers. We propose to use Haar matrix not because it is the best choice for frequency transform, but because of its simplicity for target signature features.

The Haar transform Y(K) of an K-input vector X(K) is:

$$Y(K) = H(m)X(K), \quad X(K) = H^T(m)Y(K) \tag{5}$$

where $K = 2^m$. To obtain proper averages, for H(4), first 2 rows are scaled by $1/\sqrt{16}$, next 2 by $1/\sqrt{8}$, next 4 by $1/\sqrt{4}$, and the last 8 by $1/\sqrt{2}$. Note that this operation will scale orthogonality of the matrix. We note the following:

- The first element in Y is the average (DC) value of X
- The second element is a low frequency component of the input vector X
- The next two components of Y correspond to moderate frequencies in input X
- The next four elements correspond to moderate-to-high frequency components in X, and
- The last eight elements correspond to high X frequencies.

Note that we did not specify what "low" and "high" frequencies are. We just want to indicate relative sizes of groups of frequencies which can be calculated as inverses of spatial differences.

All X(K) and Y(K) vectors can be stored into extended Target Template for each entry of Table 1. During real time operation, as JSTAR plane is scanning an area for ground targets, real time X(K) and Y(K) would be calculated for any target detected, and compared against the stored ones of Table 1, to determine specific target presence. More in Section IV.

4. TARGET SIGNATURE STATISTICS

Our aim is to devise effective statistical correlation methods.

STEP 2. Produce various statistical measures and correlations

2.1 Calculate template standard statistics and correlations for
SFs, AFs and FFs (last column in Table 1)
This is all done ahead of any real time operation

2.2 Calculate real time target statistics and correlations, same type as in Step 2.1. This is done as real target is acquired

2.3 Produce a variety of cross statistics and compare them in real time (all or selected templates vs real time signature).

In all the Steps above we treat the template and real time data as two sequences of either "independent" or "dependent" stochastic processes, on which we perform statistical testing as described bellow. Specifically, in Steps 2.1 and 2.2 we form:

Standard Statistical Features (SSFs) which is equivalent to individual components of AF vector. In this embodiment, we will use SSFs to perform individual hypothesis testing in Section 5, and the full SF, FF and AF vectors are used for correlation features, Step 2.3.

Correlation Features (CFs):

- Pearson sample correlation coefficient (p)
- Spearman rank correlation coefficient (ρ)
- Chi square test and P-value (χ^2), (P)
- Skewness measure (s)
- Sample distance (Brownian) covariance and coefficient

(V, r), two new concepts introduced recently in [27]. Standard Pearson coefficient recovers a linear relationship that may exist among two sets of data sequences, per:

$$p_{XY}=[\Sigma(X(i)-X_a)(Y(i)-Y_a)]/[\Sigma(X(i)-X_a)^2\,\Sigma(Y(i)-Y_a))^2]^{1/2} \quad (13)$$

where the sums are evaluated from 1 to K, and X_a and Y_a are mean (average) values of X(K) and Y(K) sequences. The R_{XY} coefficient ranges from -1 to 1. It has some serious limitation as far as capturing non linear and non stationary correlations, plus $p_{XY}=0$ does not imply independence in general (only for normal distributions). On the positive, the method is simple.

Spearman rank correlation tests how relationship between two variables can be described using a monotonic function (increasing or decreasing). With no repeated values, a perfect correlation +/-1 occurs when each of the variable is a perfect monotone function of the other. Ranking refers to data transformation in which numerical values are ranked by their size. The Spearman coefficient is Pearson's for the ranked entries. For a K-sample size, K X(k) row values and Y(K) are converted to ranked $X_r(K)$ and $Y_r(K)$ and ρ is computed from:

$$\rho =1- 6\Sigma d^2(i)/n(n^2-1) \quad (14)$$

where $d(i) = X_r(i)-Y_r(i)$ is the rank difference, and the sum goes from 1 to K. We can also use (13) above with $X_r(K)$ and $Y_r(K)$ instead of original samples.

Chi square test is used to test independency of the two sequences. The test returns the value from chi-squared distribution for the statistic and the degrees of freedom number. In the context of our paper, we will test independency of real time (an experiment) and template signature entries (hypothesized results). The test is defined as:

$$\chi^2=\Sigma\,(A_i-E_i)^2/E_i \quad (15)$$

where A_i=actual sample value, and E_i=expected sample value, and the sum is from 1 to K. A low value of χ^2 is an indicator of independence. As can be seen from the formula, χ^2 is always positive or 0 (only if $A_i = E_i$ for every i). Once χ^2 is calculated, an appropriate program, (e.q. Excel CHITEST) returns the probability P that a value of the χ^2 statistic at least as high as the value calculated by (15) could have happened by chance under the assumption of independence. In computing P-value, program uses χ^2 distribution with an appropriate number of degrees of freedom, df=K–1. The test is most appropriate when E_i's are not too small (≥5).

The skewness is based upon the sample formula:

$$s=(1/K)\,\Sigma(X(i)-X_a(i))^3/[(1/K-1)\,\Sigma(X(i)-X_a(i))^{3/2}] \quad (16)$$

with average value $X_a(i)$. Often another formula is used, i.e. the adjusted Fisher-Pearson standardized moment coefficient:

$$s_1=s(K^2)/(K-1)(K-2) \quad (17)$$

(SKEW in Excel). The variance from a normal distribution is:

$$Var(s_1)=6K(K-1)/(K-2)(K+1)(K+3) \quad (18)$$

Skewenss is obviously zero for any symmetric distribution.

Finally, we want to introduce a newest form of correlation [ ], i.e. distance correlation and distance covariance (equivalent to Brownian distance covariance and coefficient). The key advantage is that zero correlation implies independence, plus the coefficient captures non stationary and non linear correlations as well. Here is how it works.

For a random sample (X,Y)=[(X(k),Y(k), k=1,…,K] of K i.i.d. (independent identically distributed) vectors (X,Y) from the joint distribution of the random vectors X in R^p and Y in R^q, compute the Euclidean distance matrices:

$$[a(k,l)] = (|X(k)-X(l)|_p),\ \ [b(k,l)] = (|Y(k)-Y(l)|_q) \quad (19)$$

and then define:

$$A(k,l) = a(k,l) - a(k) - a(l) + a$$
$$B(k,l) = b(k,l) - b(k) - b(l) + b,\ \ k,l = 1,2,\ldots,K \quad (20)$$

where:

$$a(k) = (1/n)\Sigma_l\, a(k,l)$$
$$a(l) = (1/n)\Sigma_k\, a(k,l)$$
$$a(k) = (1/n^2)\Sigma_k\Sigma_l\, a(k,l) \quad (21)$$

and the sums go from 1 to K. Then, the non negative sample distance covariance is defined as:

$$V_n^2(X,Y) = (1/n^2)\Sigma_k\Sigma_l A(k,l)B(k,l)\ ,\ \ k,l = 1,2,\ldots K \quad (22)$$

and the corresponding sample distance correlation as:

$$R_n^2(X,Y) = V_n^2(X,Y)/[V_n^2(X)V_n^2(Y)]^{1/2} \quad (23)$$

whenever $V_n^2(X)V_n^2(Y)] > 0$, and $R_n^2(X,Y) = 0$, when we have $V_n^2(X)V_n^2(Y)] = 0$. Obviously, we have sample distance variance as:

$$V_n^2(X) = V_n^2(X,X) = (1/n^2)\,\Sigma_k\Sigma_l A_{kl}^2,\ \ k,l = 1,2,\ldots K \quad (24)$$

Another interesting result in is that:

$$V_n^2(X,Y) = \|f^n_{XY}(t,s) - f^n_X(t)\, f^n_Y(s)\|^2 \quad (25)$$

where f's are corresponding characteristic functions. The results in (22) and (23) turn out to be equal to Brownian (Wiener Process) distance covariance and correlation coefficient. Again consult [27]. These are very useful results, and we believe they can be applied successfully in ATR/ID environment for hypothesis testing.

5. TARGET HYPOTHESIS TESTING

STEP 3. Execute target signature hypothesis testing.

3.1 Hypothesis testing for Steps 2.1 and 2.2
3.2 Hypothesis testing for Step 2.3

We treat real time signature as "an experiment" and template data as "test" signatures to compare against. The Null Hypothesis H_0 refers to a default "no match" position that there is no relationship between two phenomena, i.e. they are independent. The $\mathbf{H_0}$ is assumed true until evidence indicates an alternative "match" $\mathbf{H}_1$ hypothesis.

Statistical hypothesis (see Figure 4) testing is defined as:

- Compute real time and template statistics and compare to produce the value $O(T_k)$ of some test T_k statistic. This could be simple variance comparison, chi square, or any other of the methods discussed earlier. Comparison may be as simple as a quotient of the two statistics or more sophisticated calculation of so called p-value. This is the probability, under H_0, of sampling a test statistic at least as extreme as the observed.

- Reject the null hypothesis, in favor of the alternative hypothesis, if and only if the compared or p-value is less than the significance level (selected probability) threshold.

In general, we will define statistical variable $\mathbf{S^{ij}}$ (target "i" and pose "j") as a weighted average of the outputs of all the statistical tests, denoted by $O(T_k)$ in Figure 4, i.e.

$$\mathbf{S^{ij}} = \sum_{k=1}^{n} a_k O(T_k) \qquad (26)$$

where a_k is TBD weight determined by experiment or extensive Monte Carlo simulation of the observed and template signatures. Hence variable $\mathbf{S^{ij}}$ determines the threshold for the H_0 acceptance or rejection. We are interested in whether the observed data is significantly different from what would be expected if the null hypothesis is true. So the main goal is to make a proper trade-off between the probability of Type I error, i.e.:

False Alarm = Declaring H_1 when H_0 holds (27)

and Type II error, the probability of:

Missed Alarm = Declaring (keeping) H_0 when H_1 holdS (28)

In the case of (27) False Alarm may result in a wrong pose angle estimate, which is not desirable. This would correspond to a target miss-association possibility. In the case of (28) Missed Alarm would result in missing to identify a right pose angle estimate. The best possible pose estimate is determined by properly choosing $\mathbf{S^{ij}}$ threshold, based on several statistical tests listed in Task 2.

If the null hypothesis is true, then we can evaluate the probability of a Type I error and this value represents our tolerance for Type I errors, i.e. of rejecting when in fact it is true. This probability provides an important design criterion for testing. Specifically, the rejection region is chosen so that the probability of Type I error is no greater than a specified level, for example 1% and 5%. An alternative approach is to ask the question: Assuming H_0 is true, what is p-value of the test statistic. If it is close to one, then there is no reason to reject the null hypothesis, but if it is small, then there is reason to reject H_0. Which way to test H_0 will be decided by Monte Carlo simulation which is outside the scope of this paper. This can be done for a specific target class case at hand.

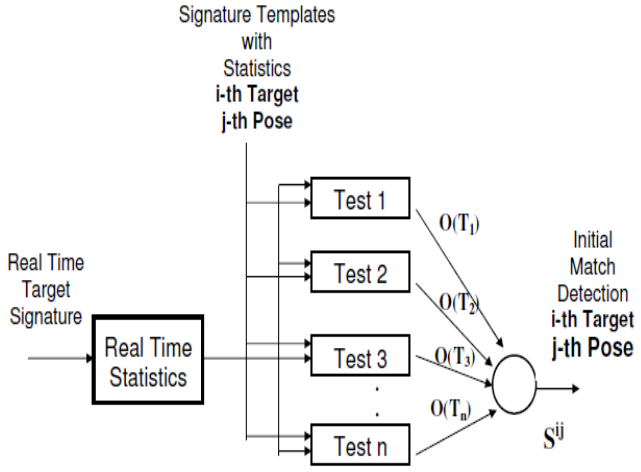

Figure 4. Forming S^{ij} Statistical Threshold

6. TARGET SIGNATURE EXAMPLE

We use Figures 2 and 3 and form specific signature features.

Spatial Features (SFs). We have the following Tables 2, 3 and 4, with N=16 discretized signature amplitudes (SFs) going from left to right, such as in Fig. 3.

TABLE 2. STATIONARY TARGET 1, SFs VECTOR $X^1_s(16)$

7	*10*	*12*	*10*	*15*	*8*	*5*	*14*	*8*	*13*	*4*	*7*	*3*	*22*	*7*	*4*

TABLE 3. MOVING TARGET 1, SFs VECTOR $X^1_m(16)$

7	*10*	*11*	*8*	*12*	*10*	*12*	*13*	*8*	*13*	*11*	*12*	*13*	*17*	*7*	*4*

TABLE 4. STATIONARY TARGET 2, SFs VECTOR $X^2_s(16)$

3	*5*	*4*	*7*	*8*	*6*	*3*	*5*	*7*	*5*	*3*	*5*	*8*	*6*	*3*	*2*

Amplitude Features (AFs). Based on Tables 2, 3 and 4, and earlier defined AF's, we have three signature results:

TABLE 5. STATIONARY TARGET 1, AFs VECTOR $A^1_s(8)$

A_{max}	A_{min}	A_{max}/A_{min}	A_{av}	A_{med}	A_{sd}	A_p	A_e
22	4	5.5	9.3125	8	4.98	6	14.9

TABLE 6. MOVING TARGET 1, AF VECTOR $A^1_m(8)$

A_{max}	A_{min}	A_{max}/A_{min}	A_{av}	A_{med}	A_{sd}	A_p	A_e
17	4	4.25	10.5	11	3.14	5	16.8

TABLE 7. STATIONARY TARGET 2, AFs VECTOR $A^2_s(8)$

A_{max}	A_{min}	A_{max}/A_{min}	A_{av}	A_{med}	A_{sd}	A_p	A_e
8	2	4	5	5	1.9	5	8.1

Frequency features (FFs). In our example, n=16, m=4, hence we need to calculate 16x16 H(4) Haar matrix which can be deduced from (3) and H(3). We have:

$H(4) = (1/\sqrt{2^4})$ times (28)

1	1	1	1	1	1	1	1	1	1	1	1	1	1	1	1

1	1	1	1	1	1	1	1	-1	-1	-1	-1	-1	-1	-1	-1
√2	√2	√2	√2	-√2	-√2	-√2	-√2	0	0	0	0	0	0	0	0
0	0	0	0	0	0	0	0	√2	√2	√2	√2	-√2	-√2	-√2	-√2
2	2	-2	-2	0	0	0	0	0	0	0	0	0	0	0	0
0	0	0	0	2	2	-2	-2	0	0	0	0	0	0	0	0
0	0	0	0	0	0	0	0	2	2	-2	-2	0	0	0	0
0	0	0	0	0	0	0	0	0	0	0	0	2	2	-2	-2
√8	-√8	0	0	0	0	0	0	0	0	0	0	0	0	0	0
0	0	√8	-√8	0	0	0	0	0	0	0	0	0	0	0	0
0	0	0	0	√8	-√8	0	0	0	0	0	0	0	0	0	0
0	0	0	0	0	0	√8	-√8	0	0	0	0	0	0	0	0
0	0	0	0	0	0	0	0	√8	-√8	0	0	0	0	0	0
0	0	0	0	0	0	0	0	0	0	√8	-√8	0	0	0	0
0	0	0	0	0	0	0	0	0	0	0	0	√8	-√8	0	0
0	0	0	0	0	0	0	0	0	0	0	0	0	0	√8	-√8

From Table 2 (stationary Target 1) we obtain corresponding frequency vector $Y^1_s(16)$ by way of H(4) and:

$$X^1_s(16) = [7,10,12,10,15,8,5,14,8,13,4,7,3,22,7,4]^T \quad (29)$$

producing:

$$Y^1_s(16) = H(4)X^1_s(16) = \quad (30)$$
$$[9.3125,0.8125,-0.375,-0.5,-1.25,1.0,2.5,3.5,-1.5,1,3.5,-4.5,-2.5,-1.5,-9.5,1.5]^T$$

If the Target 1 is moving (Table 3), we obtain the vectors:

$$X^1_m(16) = [7,10,11,8,12,10,12,13,8,13,11,12,13,17,7,4]^T$$
31)

and:

$$Y^1_m(16) = H(4)X^1_m(16) = \quad (32)$$
$$[10.5,-0.125,-1.375,0.375,-0.5,-0.75,-0.5,4.75,-1.5,1.5,1,-0.5,-2.5,-0.5,-2,1.5]^T$$

Finally, the vectors for the stationary Target 2 (Table 4) are:

$$X^2_s(16) = [3,5,4,7,8,6,3,5,7,5,3,5,8,6,3,2]^T \quad (33)$$

and

$$Y^2_s(16) = H(4)X^2_s(16) = \quad (34)$$
$$[5,0.125,-0.375,0.125,-0.75,1.5,1,2.25,-1,-1.5,1,-1,1,-1,1,0.5]^T$$

Based on the above data we form various statistics summarized in the Tables 8 and 9 bellow.

Target Scenarios / Statistical Tests		St T1	Mv T1	St T2
SFs	Mean	9.31	10.5	5
16 samples	Median	8	11	5
	St Deviation	4.9762	3.1411	1.8974
	Variance	24.7625	9.8667	3.6
	Energy	1759	1912	454
	Skewness	1.0674	-0.1475	0.1338
FFs	Mean	0.0625	0.5859	0.6406
16 samples	Median	0.0625	-0.5	0.625
	St Deviation	4.0396	3.151	1.5103
	Variance	16.3182	9.9286	2.281
	Energy	1759	1912	454
AFs	Mean	9.4585	8.315	4.3167
5 samples with median	Median	7.6667	7.375	4.5
	St Deviation	7.4365	5.4651	2.2719
	Variance	55.3107	29.8674	5.1617
	Skewness	1.6315	0.3334	0.4911

Table 8. Statistics for Step 2.1. and 2.2

Target Scenarios / Statistical Tests		St T1/St T2	St T1/Mv T1	Mv T1/St T2
SFs	Pearson Correlation	0.353	0.5864	0.4139
16 samples	Spearmen Correlation	0.925	0.936	0.9396
	Brownian Correlation	0.2653	0.354	0.2308
	Chi Square Test Prob.	2.77E-18	0.1187	9.73E-23
	Chi Square Test Value	89	33.375	87.43
	Sample Covariance	3.125	8.594	2.3125
	Brownian Covariance	1.1505	2.238	0.6382
FFs	Pearson Correlation	0.6036	0.7898	0.759
16 samples	Spearmen Correlation	N/A	N/A	N/A
	Brownian Correlation	0.4795	0.6303	0.5331
	Chi Square Test Prob.	N/A	N/A	N/A
	Chi Square Test Value	N/A	N/A	N/A
	Sample Covariance	3.453	9.425	3.386
	Brownian Covariance 1	1.034	2.371	0.8783
AFs	Pearson Correlation	0.9391	0.8968	0.9521
4 samples no median	Spearmen Correlation	0.9429	0.934	0.998
	Brownian Correlation	0.9524	0.9517	0.9997
	Chi Square Test Prob.	3.30E-07	0.3074	8.16E-05
	Chi Square Test Value	49	4.7	30.6
	Sample Covariance	11.93	27.4	9.85
	Brownian Covariance	11.6	22.6	9.62

Table 9. Statistics for Step 2.3

Some statistics, at least for this example, are more useful than others. That may translate into larger or smaller coefficients a_k in (26) or we may opt not to use some of the statistics at all. Case in point, Table 9 entry for Spearman correlation coefficient does not look useful because all three numbers are very close to each other. On the other hand, Table 9 shows that Brownian Correlation and Chi Square test give good resolution between the targets, i.e. indicating which signatures appear to be less dependent on each other and less correlated, which would support H_0 hypothesis. As the template is spanned for all targets and all pose angles, there will be a strong correlation at one

point indicating matching or H_1. In our limited size example we just wanted to indicate a possible method to find the best match between real time signature against an entry in template Table 1. As far as specific tests for defining H_0, we would look for good discrimination in offered by ratio of variances, means, energy and skewness (Table 8) and Chi Square, Brownian correlation, plus Pearson correlation, sample and Brownian covariance (Table 9). Each of these would correspond to one specific entry in S^{ij} of (26). As stated earlier we would use Monte Carlo simulation to determine specific weights a_k. For example, based on Tables 8 and 9, it appears as if more credence should be given to Chi Square and Brownian correlation compared to other methods.

At the end to summarize the results of this section, based on the statistics in Tables 8 and 9, we conclude that for the three signatures of Figure 2 both stationary and moving Target 1 show less correlation with the stationary Target 2 than to each other, which is what we would expect. We did not elaborate on usefulness of various features (SF, FF and AF), the idea was to see if for example AF would be useful in hypothesis testing. If so, and tables 8 and 9 indicate that, we would benefit from less numbers to deal with in AF compared to SF and FF. Next step would be to consider large template Table 1 and perform Monte Carlo simulation to determine coefficients a_k and $O(T_k)$ in (26). We will leave that for the follow up paper.

In any case, the outcome of all of the above is a rough estimate of the pose angle, based on the best fit between real time signature and one of the entries in signature template table. This outcome will feed into the next step, i.e. Tracking Filter which we will describe in Part II of the paper.

7. CONCLUSION

In this paper we presented a new methodology for estimating pose angle of a target with HRR or similarly generated signature. We employ a variety of local and cross statistics in spatial, frequency and amplitude domains, and then compare real time against stored template signatures. The net result is either a match (Hypothesis H_1) or a miss (Hypothesis H_0) based on statistics comparison which produces the best estimate for the pose angle.

8. REFERENCES

[1] B. Kahler and E. Blasch, Robust Multi-Look HRR ATR Investigation Through Decision - Level Fusion Evaluation", Proc. 11th International Conference On Information Fusion, July 2008.

[2] B. Kahler, J. Querns, G. Arnold, An ATR Challenge Problem Using HRR Data, Proc. SPIE, Vol. 6970, 2008.

[3] Peter S. Maybeck, Stochastic Models, Estimation, and Control, Vol. 1-3, Academic Press, 1979-1982.

[4] JSTARS- Joint Surveillance and Target Attack Radar System, USA, from The Website for Defense Industries – Air Force, December 2001.

[5] Joint STARS/JSTARS, Intelligence Resource Program, FAS Website, December 2001.

[6] J. Layne and D. Simon, A Multiple Model Estimator for a Tightly Coupled HRR Automatic Target Recognition and MTI Tracking System, SPIE Conference on Algorithms for Synthetic Aperture Radar Imagery VI, Orlando, Florida, April 1999.

[7] E. Blasch, Derivation of A Belief Filter for High Range Resolution Radar Simultaneous Target Tracking and Identification, Ph.D. Diss., Wright State University, 1999.

[8] E Blasch and C. Yang, Ten methods to Fuse GMTI and HRRR Measurements for Joint Tracking and ID", Fusion 04, July 2004.

[9] M. I. Hodzic, Estimation Algorithms for Real-Time Airborne Target, Tracking, MSc. Thesis, UB, 1985

[10] G. Minkler and J. Minkler, Theory and Application of Kalman Filtering, Magellan Book Company, 1993.

[11] M. S. Grewal, Angus P. Andrews, Kalman Filtering: Theory and Practice Using Matlab, Willey, 2001.

[12] M. I. Hodzic, Monte - Carlo Simulation of a Real Time Target Tracking Filter Operation, Informatika, 1985.

[13] M. I. Hodzic and Radovan Krtolica, Robustness of the Maneuvering Target Tracking Filters, ETAN, 1987.

[14] Y. Bar-Shalom & X. Li, Multitarget - Multisensor Tracking: Principles and Techniques, YBS, New York, 1995.

[15] E. Blasch and M. Bryant, SAR Information Exploitation Using an Information Filter Metric, IEEE, 1998.

[16] S. G. Nikolov, E. Fernandez Canga, J. J. Lewis, A. Loza, D. R. Bull, and C. N. Canagarajah, Adaptive Image Fusion Using Wavelets: Algorithms and System Design, in Multisensor Data and Information Processing for Rapid and Robust Situation and Threat Assessment, Eds. E. Lefebvre, P Valin, IOS Press, 2006.

[17] D. Gross, M. Oppenheimer, B. Kahler, B. Keaffaber, and R. Williams, Preliminary Comparison of HRR Signatures of Moving and Stationary Ground Vehicles, Proc. SPIE, Vol. 4727, 2002.

[18] H-C. Chiang, R.L. Moses, and L.C Potter, Model based classification of radar images, IEEE Transactions on Information Theory, 46, 5 (2000), 1842-1854.

[19] R. Williams, J. Westerkamp, D. Gross, and A. Palomino, Automatic Target Recognition of Time Critical Moving Targets Using 1D High Range Resolution (HRR) Radar, IEEE AES Systems Magazine, April 2000.

[20] R. Wu, Q. Gao, J. Liu, and H. Gu, ATR Scheme Based On 1-D HRR Profiles, Electronic Letters, Vol. 38, Issue 24, Nov. 2002.

[21] S. Paul, A. K. Shaw, K. Das, and A. K. Mitra, Improved HRRATR Using Hybridization Of HMM and Eigen-Template-Matched Filtering IEEE Conf. on Aco., Speech, and Sig. Proc., 2003.

[22] R.A. Mitchell and J.J. Westerkamp, Robust statistical feature based aircraft identification, IEEE Trans. Aerospace & Electronic ystems, 35, 3, 1999.

[23] E. Blasch, J.J. Westerkamp, J.R. Layne, L. Hong, F. D. Garber and A. Shaw, Identifying moving HRR signatures with an ATR Belef Filter, SPIE 2000.

[24] Chethan Parameswariah, Wavelet analysis and filters for engineering Applications, PhD Thesis, LTU, 2003

[25] E. Blasch and S. Huang, Multilevel Feature-based fuzzy fusion for target recognition, Proc. SPIE 2000.

[26] W. Snyder, G. Ettinger and S. Laprise, Modeling Performance and Image Collection Utility for Multiple Look ATR, Proc SPIE 2003.

[27] Gabor J. Szekelyi and Maria L. Rizzo, Brownian Distance Covariance, The Annals of Applied Statistics, Vol. 3, No. 4, 1236–1265, 2009

[28] F. Dicander and R. Jonsson, Comparison of Some HRR Classification Algorithms, Proc. SPIE, Vol. 4382, 2001.
[29] E. Blasch and L. Hong, Simultaneous Tracking and Identification, Conference on Decision Control, Tampa, FL, December 1998, pg. 249-256.